Supporting Information

A ratiometric fluorescent chemosensor for conveniently monitoring hydrogen sulfide concentration levels by dual fluorescence fluctuation mode of two distinct emission bands in living cells and zebrafish

Yunzhen Yang, Longwei He, Kaixin Xu and Weiying Lin*

Institute of Fluorescent Probes for Biological Imaging, School of Materials Science and Engineering, School of Chemistry and Chemical Engineering, University of Jinan, Shandong 250022, P.R. China.

Correspondence to E-mail: weiyinglin2013@163.com

Table of content

Materials and instruments

Mass spectra were performed using an LCQ Advantage ion trap mass spectrometer from Thermo Finnigan; High resolution mass spectrometric (HRMS) analyses were measured on a Finnigan MAT 95 XP spectrometer; NMR spectra were recorded on an INOVA-400 spectrometer (400 MHz), using TMS as an internal standard; Electronic absorption spectra were obtained on a LabTech UV Power spectrometer; Photoluminescent spectra were recorded with a HITACHI F4600 fluorescence spectrophotometer; The optical density was measured by a Thermo Scientific Multiskan FC microplate reader in cytotoxicity assay; The fluorescence imaging of cells was performed with Nikon A1MP confocal microscope; The pH measurements were carried out on a Mettler-Toledo Delta 320 pH meter; TLC analysis was performed on silica gel plates and column chromatography was conducted over silica gel (mesh 200–300), both of which were obtained from the Qingdao Ocean Chemicals. Except artificial synthesis of compounds **NapN$_3$**, **PCM** and **NapN$_3$-PCM**, all reagents were purchased from commercial chemical or biological reagent companies and used without further purification. For example, beta-Alanine, 4'-piperazinoucetophenone, amino acid, 4-Bromo-1, 8-naphthalic anhydride, NaSH, CH_3COOK, $AlCl_3$, K_2CO_3, 30% H_2O_2 and 8-Hydroxyjulolidine-9-aldehyde were purchased from Energy Chemical. In this research report, all instruments are listed in the support information.

Bioimaging of distinguishing H_2S levels in living cells

The cell imaging experiments were divided into two group, control and experimental, respectively. The cells were incubated with free **NapN$_3$-PCM** for 20 min, which were used as a control group. In the experimental groups, HeLa cells were incubated with **NapN$_3$-PCM** (5 μM) for 20 min, followed by treatment with H_2S (10, 25, 50, 100, 250, 500 μM) for 20 min, and then washed by PBS buffer before imaging. Cell imaging was performed by a confocal microscope with an excitation filter of 405

nm and 561 nm, the collection wavelength range is from 500-550 nm (green channel) to 570-620 nm (red channel). The ratiometric images were obtained by the images of green channel dividing to the images of red channel.

Bioimaging of distinguishing H_2S levels in zebrafish

The zebrafish imaging experiments were divided into control and experimental groups, 5-day-old zebrafish was chosen as the imaging samples. As the control group, zebrafish were incubated with **NapN_3-PCM** (5 μM) for 30 min. As the experimental groups, zebrafish were preincubated with **NapN_3-PCM** (5 μM) for 30 min, followed by treatment with H_2S (10, 25, 50, 100, 250, 500 μM) for 30 min, and then washed by PBS buffer before imaging. The confocal microscopic imaging uses Nikon A1MP confocal microscope with an excitation filter of 405 nm and 561 nm, the collection wavelength range is from 500-550 nm (green channel) to 570-620 nm (red channel). The ratiometric images were obtained by the images of green channel dividing to the images of blue channel.

Quantum yields

The fluorescence quantum yields can be calculated by means of equation (1):

$$\Phi_s = \Phi_r \left(\frac{A_r(\lambda_r)}{A_s(\lambda_s)} \right) \left(\frac{n_s^2}{n_r^2} \right) \frac{F_s}{F_r} \qquad (1)$$

Where the subscripts *s* and *r* refer to the sample and the reference, respectively. Φ, *F*, A and n stands for is quantum yield, the integrated emission intensity, the absorbance and refractive index, respectively. Fluorescein (Φ=0.95) in 0.1 M NaOH solution and Rhodamine B (Φ=0.31) [3-4] in water were used as the standard for calculating fluorescence quantum yields of Nap and PCM moiety, respectively.

Synthesis

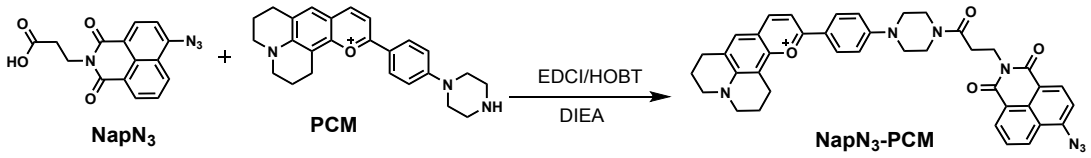

Scheme S1. Synthesis of chemosensor **$NapN_3$-PCM**.

Synthesis of compounds **$NapN_3$** and **PCM** were prepared via previous procedure.[1-2] The target mixture containing **$NapN_3$-PCM** was readily synthesized in one simple step. As shown in Scheme S1, the compound 31 mg of **$NapN_3$** (0.1 mmol), 65 mg of **PCM** (0.2 mmol), 32.5 mg of EDCI (0.2 mmol) and 10.5 mg of HOBT (0.01 mmol) were added to a 50 mL reaction bottle. The mixture was dissolved in 4 mL CH_2Cl_2 under N_2 atmosphere and dark. Then, the mixture was refluxed at room temperature overnight. After solvent evaporation, the crude product was purified by silica gel column chromatography using CH_2Cl_2/MeOH (v/v 30:1) and product **$NapN_3$-PCM** (49 mg) was obtained as a purple solid in 72.24% yield. ^{1}H NMR (400 MHz, DMSO-d6) δ 1.23 (s, 4H), 1.94-2.01 (d, *J* = 27.6 Hz, 4H), 2.76-2.80 (t, *J* = 7.6 Hz, 2H), 2.84-2.86 (t, *J* = 5.2 Hz, 2H), 2.96-2.99 (t, *J* = 5.6 Hz, 2H), 3.56-3.63 (d, *J* = 28.4 Hz, 8H), 4.24-4.28 (t, *J* = 8.0 Hz, 2H), 7.11-7.14 (d, *J* = 9.2 Hz,2H), 7.48 (s, 1H), 7.72-7.74 (d, *J* = 8.0 Hz,1H), 7.78-7.80 (d, *J* = 8.4 Hz, 1H), 7.84-7.88 (d, *J* = 8.0 Hz, 1H), 8.05-8.08 (t, *J* = 8.8 Hz, 2H), 8.37-8.43 (dd, *J* = 14.0 Hz, 8.4 Hz 2H), 8.45-8.47 (d, *J* = 8.0 Hz, 1H), 8.51-8.53 (d, *J* = 7.2 Hz, 1H); ^{13}C NMR (100 MHz, DMSO-d6) δ 12.93, 17.22, 18.57, 19.28, 19.46, 20.30, 27.45, 31.44, 36.74, 42.32, 44.50, 46.12, 46.43, 50.37, 50.86, 54.09, 104.89, 107.17, 114.20, 116.29, 117.19, 118.42, 122.42, 123.86, 127.24, 127.70, 128.61, 128.82, 130.09, 131.98, 143.26, 146.08, 151.72, 152.97, 154.20, 163.07, 163.53, 165.26, 169.35. HRMS (ESI) *m/z* calcd for $C_{40}H_{36}N_7O_4$ (M^+): 678.2829. Found 678.2831.

Table S1. Summary of the properties of representative fluorescent H_2S chemosensors reported previously and chemosensor $NapN_3$-PCM introduced in this work.

Chemosensor	Chemical structures	Number of recognition sites	The type of Fluorescent signal	Emission wavelengths	References
ESIPT-HS	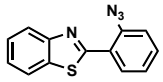	1	Turn on	450 nm	5
SF2	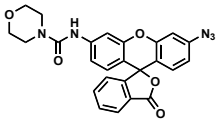	1	Turn on	525 nm	6
1	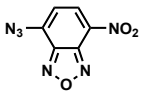	1	Turn on	550 nm	7
Lyso-AEP	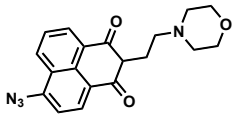	1	Turn on	535 nm	8
AZMB-Coumarin	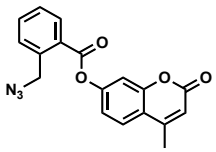	1	Turn on	450 nm	9
NI-NHS	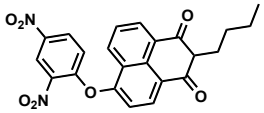	1	Turn on	550 nm	10
NR-HS	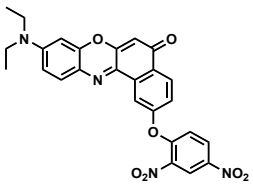	1	Turn on	538 nm	11

NBD-Coum	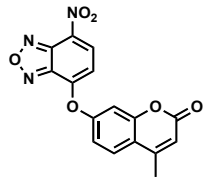	1	Turn on	449 nm	12
L	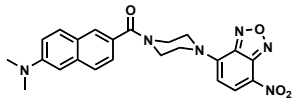	1	Turn on	488 nm	13
L	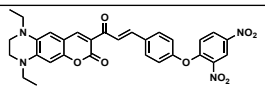	1	Turn on	488 nm	14
CouMC	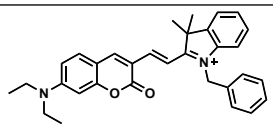	1	Antagonistic ratiometric	485/690 nm	15
TR-H_2S	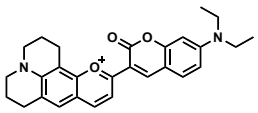	1	Antagonistic ratiometric	487/707 nm	16
WPS2	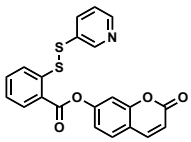	1	Turn on	456 nm	17
SFP-2	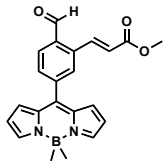	1	Turn on	510 nm	18
HS-Cy	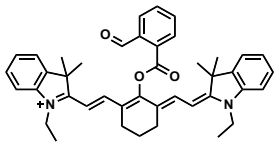	1	Antagonistic ratiometric	625/780 nm	19
1	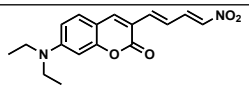	1	Antagonistic ratiometric	511/650 nm	20
NSN1	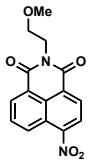	1	Turn on	542 nm	21

1	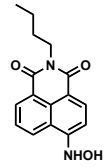	1	Turn on	544 nm	22
CP-H_2S	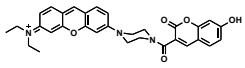	1	Antagonistic ratiometric	454/573 nm	23
CN-N_3	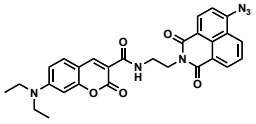	1	Antagonistic ratiometric	474/534 nm	24
NapN_3-PCM	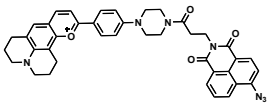	2	Synergistic and antagonistic ratiometric	535/650 nm	This work

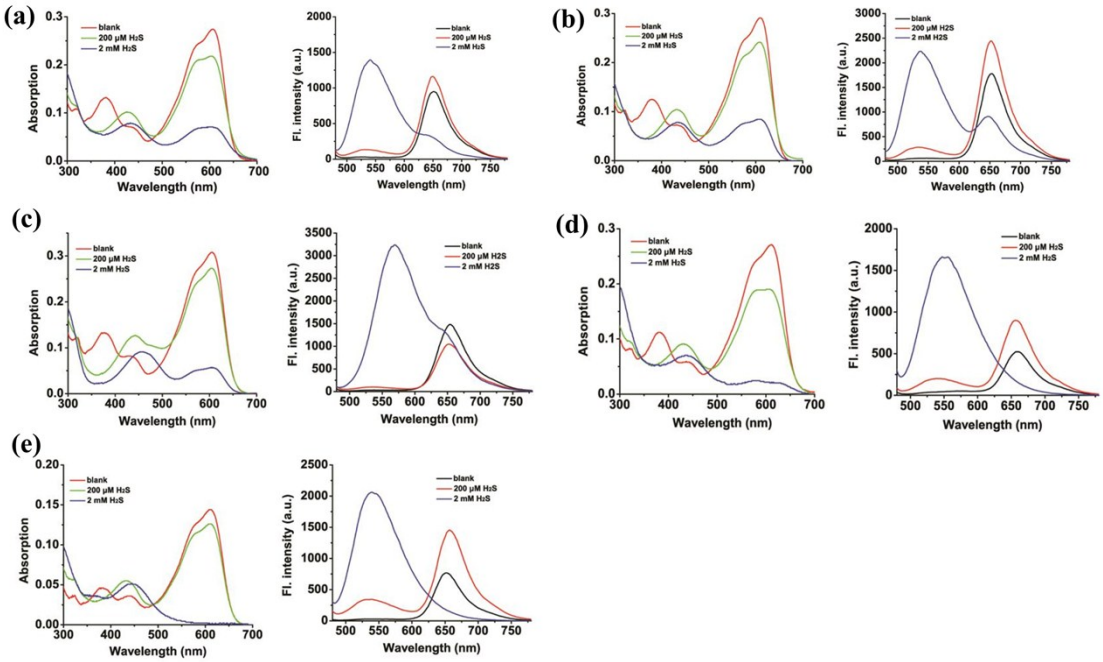

Fig. S1. The UV (left) and fluorescence (right) spectra of **NapN$_3$-PCM** in the absence or presence of 200 μM and 2 mM NaHS in PBS buffer (25 mM, pH 7.4) containing 50% (a) MeOH, (b) EtOH, (c) MeCN, (d) DMSO, and (e) DMF. Excition at 445 nm for fluorescence spectra.

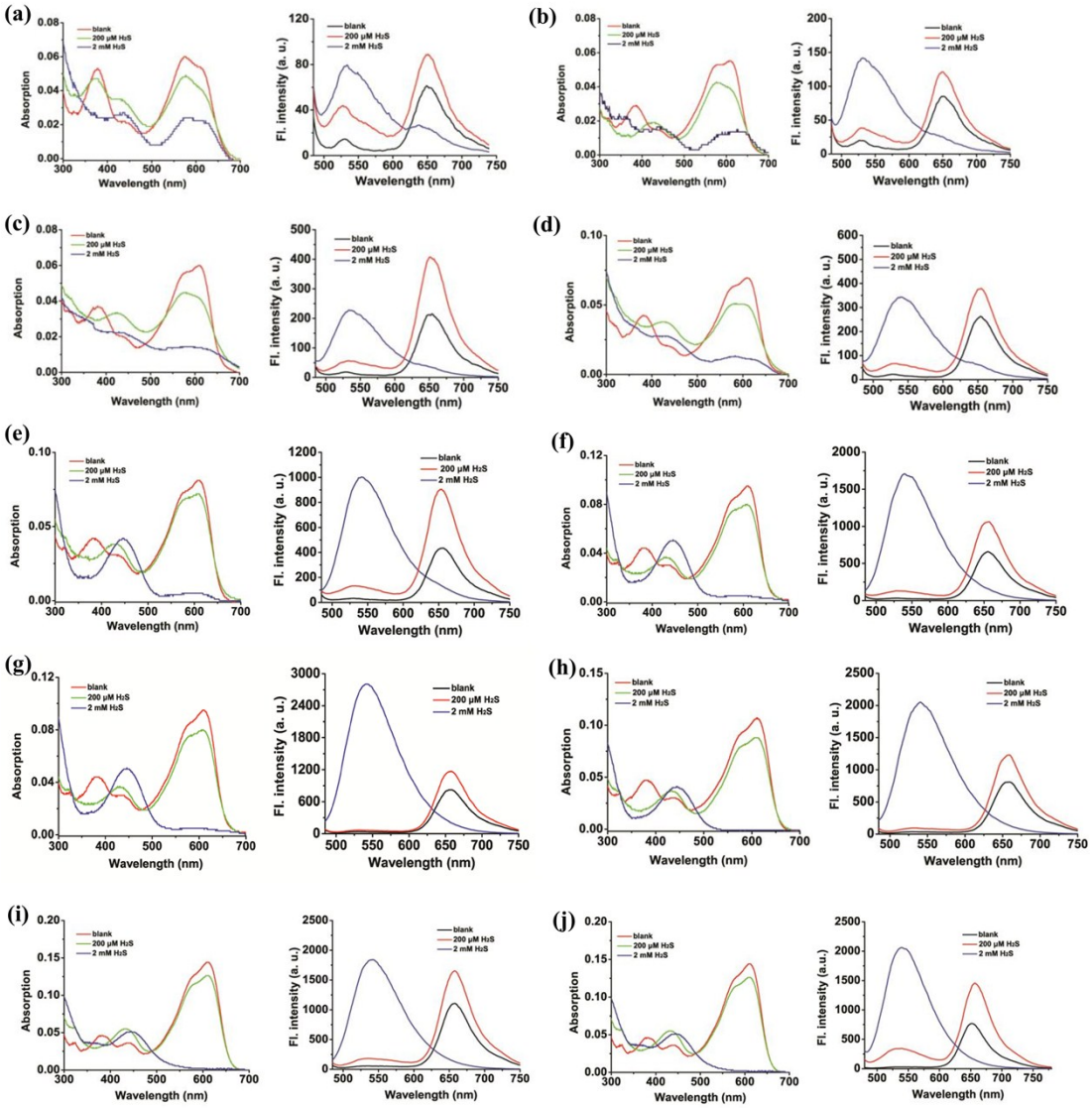

Fig. S2. The UV (left) and fluorescence (right) spectra of **NapN_3-PCM** in the absence or presence of 200 μM and 2 mM NaHS in PBS buffer (25 mM, pH 7.4) containing (a) 5%, (b) 10%, (c) 15%, (d) 20%, (e) 25%, (f) 30%, (g) 35%, (h) 40%, (i) 45%, and (j) 50% DMF. Excition at 445 nm for fluorescence spectra.

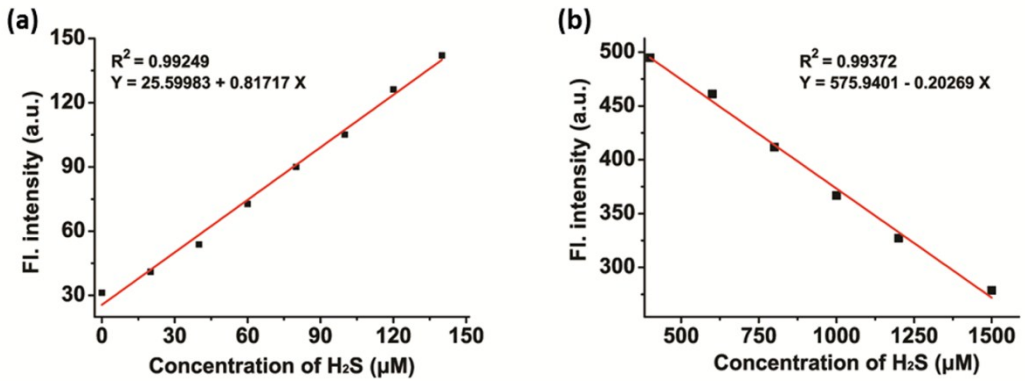

Fig. S3 (a) The linear relationship between of fluorescence intensity and the concentration of H_2S (20-150 μM). (b) The linear relationship between of fluorescence intensity and the concentration of H_2S (400-1500 μM).

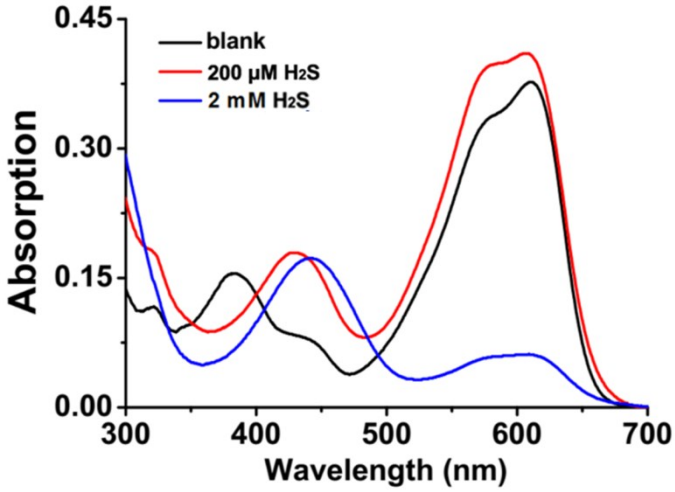

Fig. S4 Absorption spectra of **NapN$_3$-PCM** in the absence or presence of 200 μM and 2 mM NaHS in PBS buffer (25 mM, pH 7.4, containing 25% DMF).

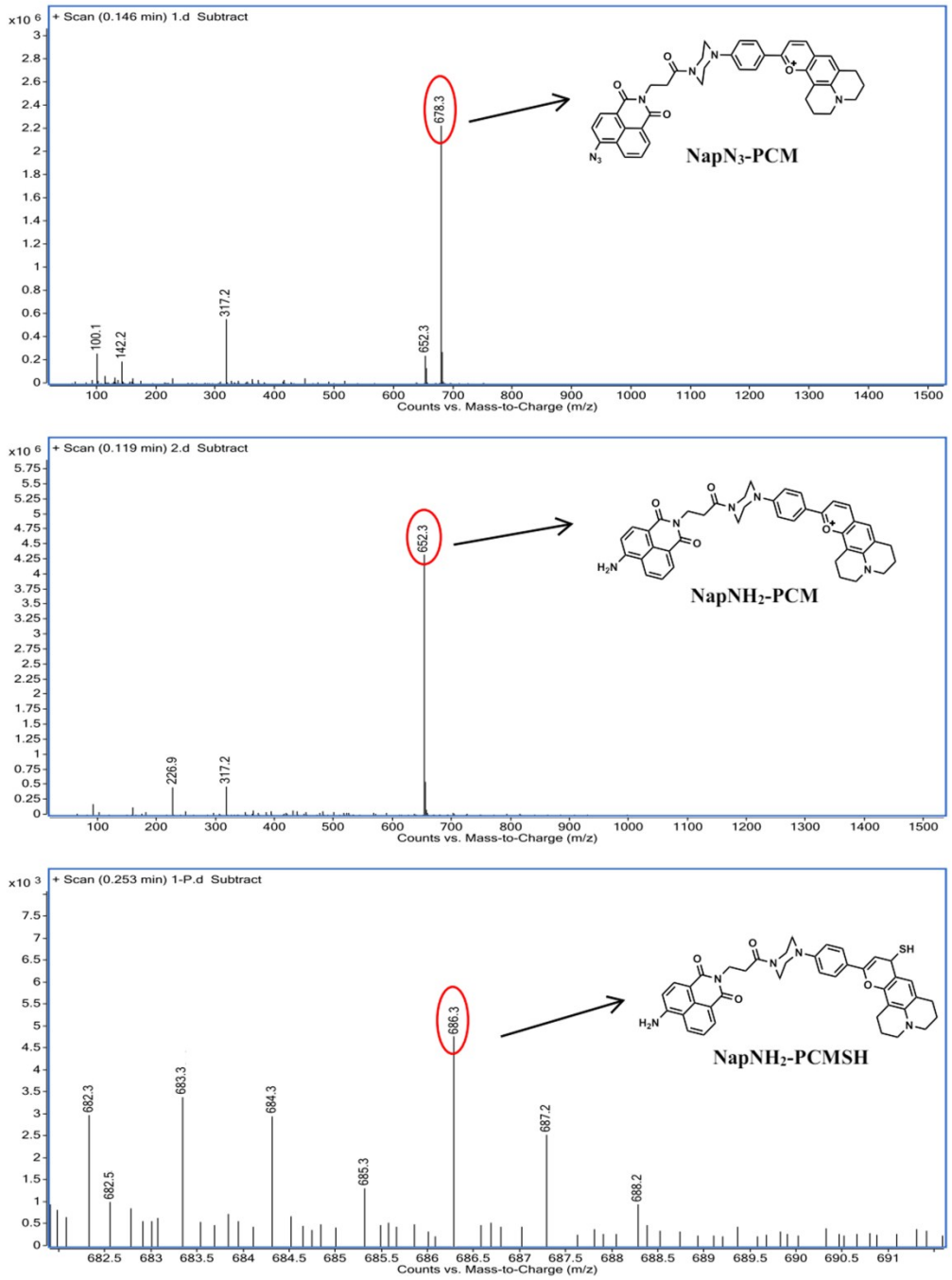

Fig. S5 Mass spectra (ESI) of **$NapN_3$-PCM** in the absence (above) or presence of 200 μM (middle) and 2 mM NaHS (bottom) in aqueous solution.

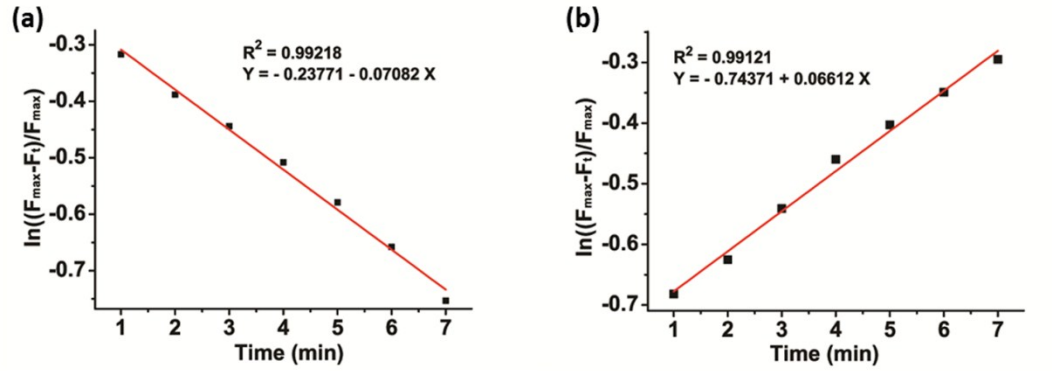

Fig. S6 Pseudo first-order kinetic plot of the reaction of **NapN$_3$-PCM** (10 μM) with NaSH (200 μM) in aqueous solution (25 mM PBS buffer, pH 7.4, mixed with 25% DMF). Slope = 0.07082 min^{-1}. (b) Pseudo first-order kinetic plot of the reaction of **NapN$_3$-PCM** (10 μM) with NaHS (2 mM) in aqueous solution (25 mM PBS buffer, pH 7.4, mixed with 25% DMF). Slope = 0.06612 min^{-1}

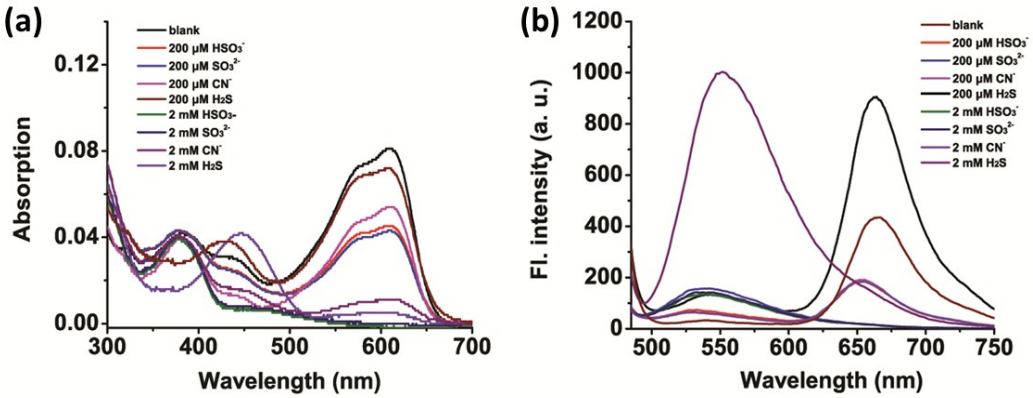

Fig. S7 (a) Absorption and (b) emission spectra of **NapN$_3$-PCM** in the absence or presence of 200 μM or 2 mM HSO_3^-, SO_3^{2-}, CN^- in PBS buffer (25 mM, pH 7.4, containing 25% DMF).

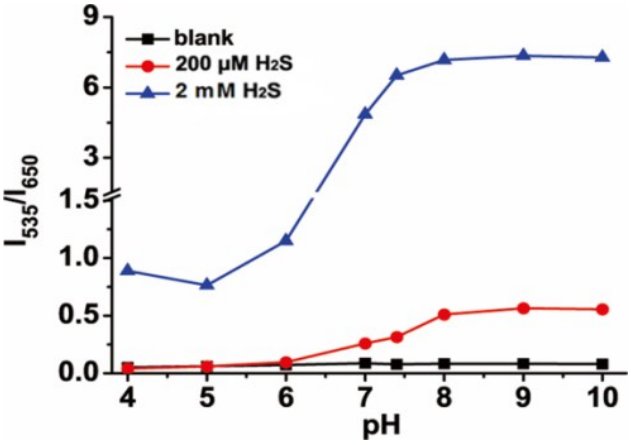

Fig. S8 The ratio values of fluorescence intensity of **NapN$_3$-PCM** (10 μM) at 535 nm and 650 nm in the presence or absence of 200 μM (red) or 2 mM (blue) H2S in various pH ranging from 4.0 to 10.0 in 25Mm PBS buffer (containing 25% DMF), respectively.

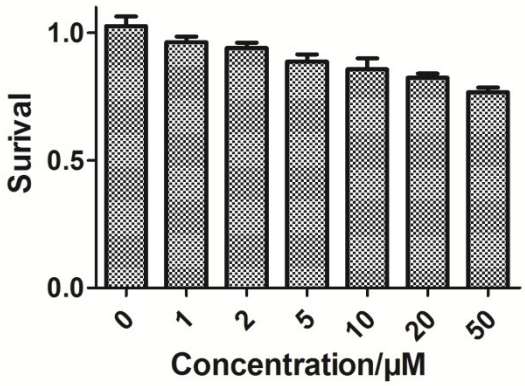

Fig. S9 cell viability of HeLa cells incubated with chemosensor **NapN$_3$-PCM** of different concentration (0, 1, 2, 5, 10, 20, or 50 μM) for 24 h.

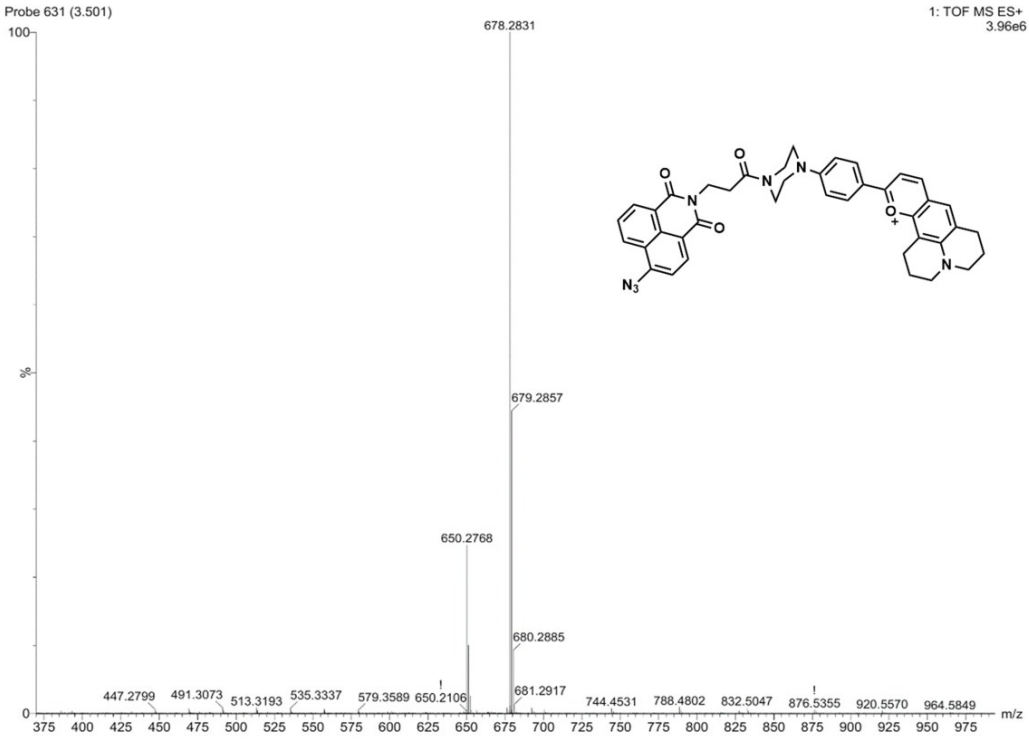

Fig. S10 HRMS (ESI) of compound **NapN_3-PCM** m/z calcd for $C_{40}H_{36}N_7O_4$ (M^+): 678.2829. Found 678.2831.

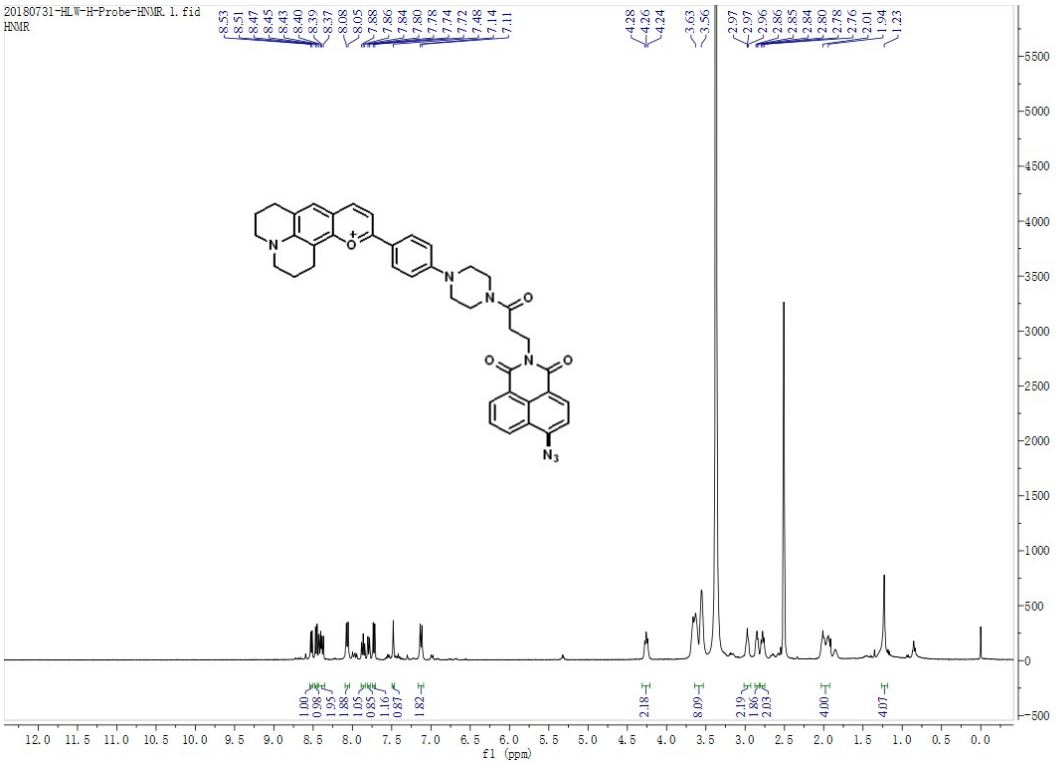

Fig. S11 ^{1}H NMR spectrum of compound **NapN_3-PCM** in DMSO.

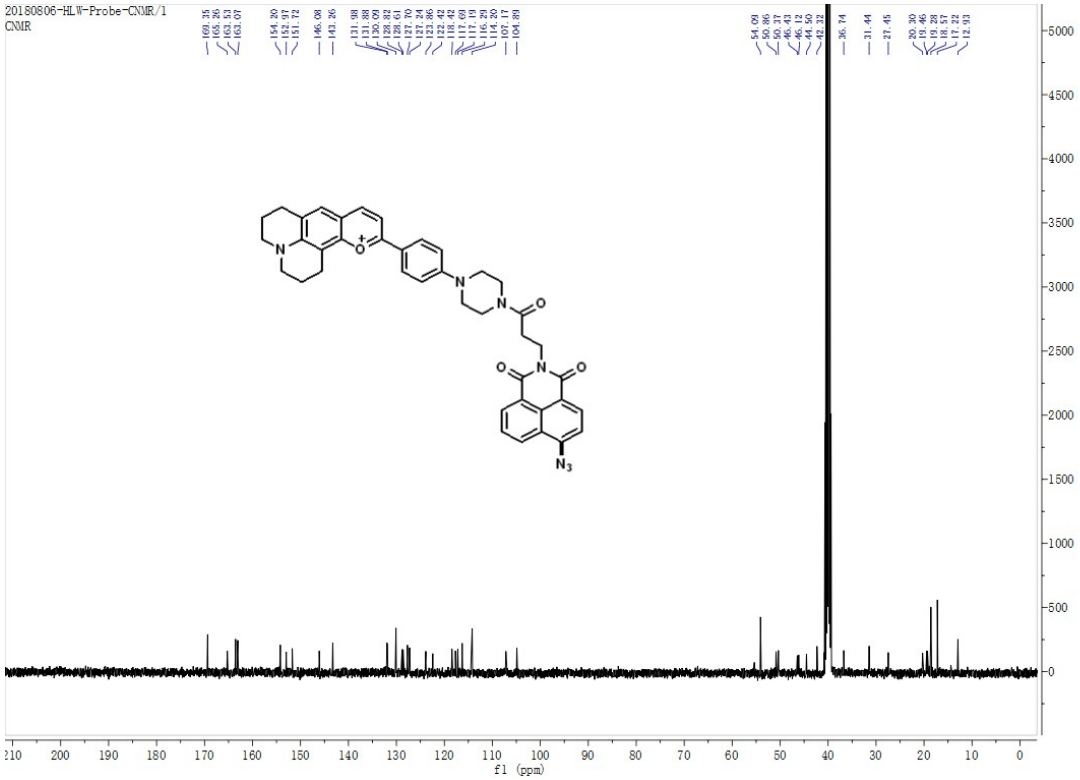

Fig. S12 ^{13}C NMR spectrum of compound **NapN_3-PCM** in DMSO.

References

1 M. Singha, S. Roy, S. D. Pandey, *Chem. Commun.*, 2017, **53**, 13015-13018.

2 L. He, X. Yang, K. Xu, *Chem. Commun.*, 2017, **53**, 13168-13171.

3 H. Li, X. Li, W. Shi, Y. Xu and H. Ma, *Angew. Chem.,* 2018, **57**, 12830-12834.

4 L. He, W. Lin, Q. Xu, and H. Wei, *ACS Appl. Mater. Interfaces,* 2014, **6**, 22326−22333

5 J. Zhang and W. Guo, *Chem. Commun.,* 2014, **50**, 4214-4217.

6 A. R. Lippert, E. J. New and C. J. Chang, *J. Am. Chem. Soc.,* 2011, **133**, 10078–10080.

7 G. Zhou, H. Wang, Y. Ma and X. Chen, *Tetrahedron*, 2013, **69**, 867-870.

8 Q. Qiao, M. Zhao, H. Lang, D. Mao, J. Cui and Z. Xu, *RSC Adv.,* 2014, **4**, 25790-25794.

9 Z. Wu, Z. Li, L. Yang, J. Han and S. Han, *Chem. Commun.,* 2012, **48**, 10120-10122.

10 T. Liu, X. Zhang, Q. Qiao, C. Zou, L. Feng, J. Cui and Z. Xu, *Dyes Pigm.,* 2013, **99**, 537-542.

11 Y. Liu and G. Feng, *Org. Biomol. Chem.,* 2014, **12**, 438-445.

12 M. D. Hammers and M. D. Pluth, *Anal. Chem.,* 2014, **86**, 7135.

13 Y. Tang and G. F. Jiang, *New J. Chem.,* 2017, **41**.6769-6774.

14 C. F. Wang, X. X. Cheng, H. J. Zhang and X. J. Zhang, *Chem. Sci.,* 2018, **9**, 8369–8374.

15 J. Liu, Y.-Q. Sun, J. Zhang, T. Yang, J. Cao, L. Zhang and W. Guo, *Chem. – Eur. J.,* 2013, **19**, 4717-4722.

16 H. D. Li, Q. C. Yao, J. L. Fan, N. Jiang, J. Y. Wang, J. Xiab and X. J. peng, *Chem. Commun.*, 2015, **51**, 16225-16228.

17 B. Peng, W. Chen, C. Liu, E. W. Rosser, A. Pacheco,Y. Zhao, H. C. Aguilar and M. Xian, *Chem. – Eur. J.,* 2014, **20**, 1010.

18 Y. Qian, J. Karpus, O. Kabil, S.-Y. Zhang, H.-L. Zhu, R. Banerjee, J. Zhao and C. He, *Nat. Commun.,* 2011, **2**, 495-501.

19 X. Wang, J. Sun, W. Zhang, X. Ma, J. Lv and B. Tang, *Chem. Sci.,* 2013, **4**, 2551-2556

20 M. Wu, K. Li, J. Hou, Z. Huang and X. Yu, *Org. Biomol. Chem.,* 2012, **10**, 8342–8347.

21 L. A. Montoya and M. D. Pluth, *Chem. Commun.,* 2012, **48**, 4767–4769.

22 W. Xuan, R. Pan, Y. Cao, K. Liu and W. Wang, *Chem. Commun.,* 2012, **48**, 10669–10671.

23 L. He, X. Yang, Y. Liu and W. Lin, *Anal. Methods,* 2016, **8**, 8022-8027.

24 . L. He, W. Lin, Q. Xu and H. Wei, *Chem. Commun,* 2015,**51**, 1510-1513.